Journal of Power Sources 218 (2012) 375–382

Contents lists available at SciVerse ScienceDirect

Journal of Power Sources

journal homepage: www.elsevier.com/locate/jpowsour

Impacts of operating conditions on the effects of chloride contamination on PEM fuel cell performance and durability

Hui Li [a], Shengsheng Zhang [a], Weimin Qian [a], Yi Yu [a], Xiao-Zi Yuan [a], Haijiang Wang [a,*], Max Jiang [a], Silvia Wessel [b], Tommy T.H. Cheng [b]

[a] National Research Council of Canada, Vancouver BC, Canada V6T 1W5
[b] Ballard Power Systems Inc., Burnaby BC, Canada V5J 5J8

HIGHLIGHTS

- Fuel cell contamination tests were conducted by injecting ppm levels of chloride into the air stream.
- Effect of various operating conditions on chloride contamination was studied.
- In-situ diagnosis was performed to investigate the chloride contamination impacts and mechanisms.

ARTICLE INFO

Article history:
Received 17 April 2012
Received in revised form
28 June 2012
Accepted 1 July 2012
Available online 7 July 2012

Keywords:
Charge transfer
Chloride contamination
Electrochemical surface area
Mass transfer
PEM fuel cells

ABSTRACT

Chloride contaminated fuel and/or air streams in an operating proton exchange membrane fuel cell can cause significant adverse effects on fuel cell performance and durability. This paper reports investigations of chloride contamination effects on PEM fuel cell performance and durability under a wide range of operating conditions, using various in-situ diagnostic measurements. Increases in current density and Cl^- concentration as well as decreases in fuel cell RH were found to enlarge the severity of the chloride contamination effect. Temperature was also found to have a significant influence on the contamination effect.

Electrochemical impedance spectroscopy was used as a diagnostic tool during the contamination tests to explore changes in cell component resistances. The results indicated that chloride contamination causes predominantly an increase in charge transfer resistance as well as an increase in mass transfer resistance. The membrane resistance was not found to be impacted by chloride contamination. As measured by cyclic voltammetry, the presence of chloride in the air stream significantly reduced the cathode electrochemical surface area, and this reduction is believed to be due to the adsorption of chloride on the Pt surface causing active site blockage and accelerated Pt dissolution and agglomeration via the formation of Pt–Cl complexes.

1. Introduction

Due to its high efficiency, environmental friendliness, and modularity, the proton exchange membrane fuel cell (PEMFC) is widely believed to be the most attractive candidate for both transportation and stationary power generation in the near future. During the last several decades, intensive efforts have been made to optimize the cell components/system design to pursue a substantial improvement in both performance and durability. Currently, more durable fuel cells with higher performance are being produced based on a more profound understanding of their operational behaviour and degradation mechanisms. In addition to the components/system level of efforts, one critical area of interest is the effects of contamination caused by impurities in the feed streams or from cell components during operation, since contamination can cause severe fuel cell degradation or failure under actual operating conditions [1].

Recently, the poisoning effect of chloride on PEMFC performance and durability has received much research attention. Chloride is present in the atmosphere as an aerosol in coastal areas and as a de-icer on roads during the winter time [2]. Trace amounts of chloride may also arise from catalyst preparation due to the use of platinum chloride precursors during catalyst synthesis. Moreover, chloride is also a likely contaminant in the water contained in the feed streams of PEMFCs [3]. As a result, some research efforts have been made in

* Corresponding author. Tel.: +1 6042213038; fax: +1 6042213001.
E-mail address: haijiang.wang@nrc-cnrc.gc.ca (H. Wang).

0378-7753/$ – see front matter
http://dx.doi.org/10.1016/j.jpowsour.2012.07.003

recent years to study the effects of chloride being present in the air stream in an operating fuel cell [4,5]. Some ex-situ studies have also been conducted to study the adsorption of chloride on the Pt surface and the effects of chloride on the kinetics and mechanisms of the oxygen reduction reaction (ORR), using rotating ring-disk electrode (RRDE) [3], electrochemical quartz crystal microbalance (EQCM) [6,7], and inductively coupled plasma (ICP)-mass analysis in combination with atomic force microscopy (AFM) [7].

In addition to the chloride present in the air stream, as described in detail in our previous publication [8], the direct use of waste or by-product hydrogen from chemical plants (e.g., in the chlor-alkali industry) to reduce hydrogen production and transportation costs requires the understanding of the impacts of chlorine on PEMFC performance and durability [8]. Through the examination of the speciation of chlorine, it was concluded in our previous publication that chlorine would react with hydrogen to produce hydrogen chloride, which is the most favorable species in the presence of catalyst Pt in the anode environment of the fuel cell. Additionally, the preliminary investigations of chloride contamination with regards to its poisoning behaviour and mechanisms, which included the effects of the injection side (anode vs. cathode injection) and HCl concentration in the fuel stream (as high as 20 ppm), were conducted [8]. It was concluded that cell voltage during chloride contamination was characterized by an initial sudden drop (e.g., around 120 mV at 1.0 A cm^{-2} with 4 ppm HCl injected from the fuel side), followed by a plateau (steady-state). It was also concluded that, other than a delayed sudden drop observed during fuel-side injection, the injection side of HCl did not lead to much difference in the sudden voltage drop or in the steady-state cell performance loss. Furthermore, regardless of the injection side, the cathode, rather than the anode side, suffered losses in electrochemical surface area (ECSA). The results suggested that chloride contamination is predominantly a cathode effect.

In addition to the in-situ studies, we also examined the effects of ppm levels of chloride ions on a carbon-supported Pt catalyst using the EQCM method [9]. It was found that the dissolution of Pt particles and the adsorption of chloride ions resulted in ECSA losses, which was in agreement with the conclusions drawn from our in-situ studies [8].

In this present investigation, following our previous studies on chloride contamination [8,9], we studied the chloride contamination effects at different chloride concentrations and under different operating conditions. The objectives of the current study were to further examine the threshold level of chloride contamination and the effects of operating conditions (temperature and relative humidity (RH)) on the chloride poisoning behaviour. The investigation was conducted by evaluating the direct effect of HCl on cell performance and durability and through various diagnostic measurements.

2. Experimental

2.1. Experimental setup

The configuration of the contamination testing platform is similar to that reported in our previous publication [8]. Since no significant difference was found between anode and cathode injection, all contamination tests were conducted with the HCl being injected from the cathode side through the air stream in this investigation. The contaminant level was relative to the air flow rate, and controlled by the concentration of the HCl solution stored in a liquid reservoir and the pumping rate of the high-pressure pump. The amount of water introduced with HCl injection was compensated for by adjusting the dew point so that the desired RH in the cell was maintained. As described previously, various anti-corrosion measures were taken to avoid any other potential impurities resulting from hardware corrosion by HCl.

A Teledyne Medusa RD fuel cell test station was employed for controlling gas flows and dew points (the temperatures of the humidifier), and a Teledyne single-cell hardware with gold-coated end plates was used. The membrane electrode assembly (MEA), with an active area of 50 cm^2, consisted of SGL gas diffusion layers (GDLs) with 20% PTFE loading and Gore PRIMEA® series 5710 catalyst coated membrane (CCM). The catalyst loadings were 0.4 and 0.1 mg Pt cm^{-2} for the cathode and anode, respectively. A fresh MEA was employed for each contamination test.

2.2. Diagnostic measurements

The main diagnostic measurements during the tests were electrochemical impedance spectroscopy (EIS), cyclic voltammetry (CV), and linear sweep voltammetry (LSV). The EIS tests were performed using the integrated frequency response analyzer of the Teledyne test station over the 3000–0.1 Hz range. CV and LSV tests were performed using a Solartron 1287 potentiostat to evaluate the ECSA of the cathode catalyst layers (CCLs) and the hydrogen crossover current of the membrane. During the CV and LSV measurements, the cathode was fed with N_2 and acted as the working electrode, while the anode was fed with H_2 and acted as the reference electrode.

2.3. Testing conditions

Using the Teledyne test station, all contamination tests were conducted in a constant current discharge mode. The first set of contamination tests, with the aim to gauge the effects of HCl concentration, were conducted with three concentrations of HCl at two current densities, with the lowest concentration being 0.1 ppm. Secondly, the contamination tests were carried out at various RHs and temperatures to explore the effects of these operating conditions on the severity of the HCl contamination effect. In all contamination tests, the EIS measurements were performed at regular intervals throughout the test, while the CVs were only performed at the beginning of test (BOT) and the end of test (EOT) so that the contamination process was not interrupted. Lastly, a contamination test with middle of test (MOT) diagnostics, intended to investigate how the presence of HCl affects the ECSA and open current voltage (OCV) with progressive contamination, was also carried out with EIS, OCV, and CV performed at regular intervals during the test.

For all contamination tests, the stoichiometries of hydrogen and air were kept at 1.5/2.5, respectively, and the inlet pressure was 25 psig. Other conditions, varied depending on the purpose of the tests, are listed in Table 1.

3. Results and discussion

3.1. Effect of HCl concentration

As mentioned earlier, the effects of higher HCl contamination levels (such as 20 and 4 ppm) on fuel cell performance were studied in our previous publication [8]. The main objective of the presented

Table 1
Operating conditions for the contamination tests.

Name of test	HCl level (ppm)	RH (%)	Temperature (°C)	Current density (A cm^{-2})
Effect of concentration 1	4, 1, 0.1	100	80	1.0
Effect of concentration 2	4, 2, 0.1	100	80	0.75
Effect of RH	4	40, 60, 80, 100	80	1.0
Effect of temperature	4	80	40, 60, 80	1.0
Test with MOT diagnostics	2	80	80	0.75

work was to evaluate the effects of much lower HCl levels with the aim to determine the threshold contamination levels of HCl in the feed stream. Therefore, the effects of HCl concentration, as low as 0.1 ppm, were investigated at two current densities, 1.0 and 0.75 A cm^{-2}.

3.1.1. Cell voltage vs. time

Fig. 1 shows the behaviour of cell voltage vs. time collected during the contamination tests with various HCl concentrations (note: the large voltage increase during the 4 ppm HCl contamination test at 0.75 A cm^{-2} was a recovery test). It can be seen that, with the HCl concentrations of 1 or 4 ppm, a sudden drop followed by a plateau was observed at both current densities. However, when the HCl concentration was as low as 0.1 ppm, there was no sudden drop during the contamination process, although the linear cell performance degradation rates were faster than those of the baselines without contaminant (0.17 vs. 0.11 mV h^{-1} at 1.0 A cm^{-2}, and 0.10 vs. 0.04 mV h^{-1} at 0.75 A cm^{-2}). The absence of a sudden drop during contamination tests with 0.1 ppm HCl suggests that the degree of contamination is very close to the threshold level of HCl contamination. This notion was further supported by the EOT polarization curves in Fig. 2. In agreement with the behaviour of cell voltage vs. time, the presence of 0.1 ppm HCl was found to have minimal impact on cell polarization.

Fig. 3 summarizes the sudden voltage drop (obtained from Fig. 1) as a function of HCl concentration at the two current densities. As expected, the sudden voltage drop in fuel cell performance increased with increasing HCl concentration. In addition, the increase in current density from 0.75 to 1.0 A cm^{-2} also boosted the HCl contamination effect significantly. The effect of current density on the severity of HCl contamination can be attributed to two competing factors: (1) chloride dosage and (2) water generation. As current density increases, the chloride dosage increases due to the higher air flow rate that brings more chloride into the system at higher current density, which would increase the chloride contamination effect. On the other hand, when current density increases, more water is generated, thus reducing the chloride contamination effect. The greater performance loss observed at 1.0 A cm^{-2} vs. 0.75 A cm^{-2} suggests that the dosage effect is dominant.

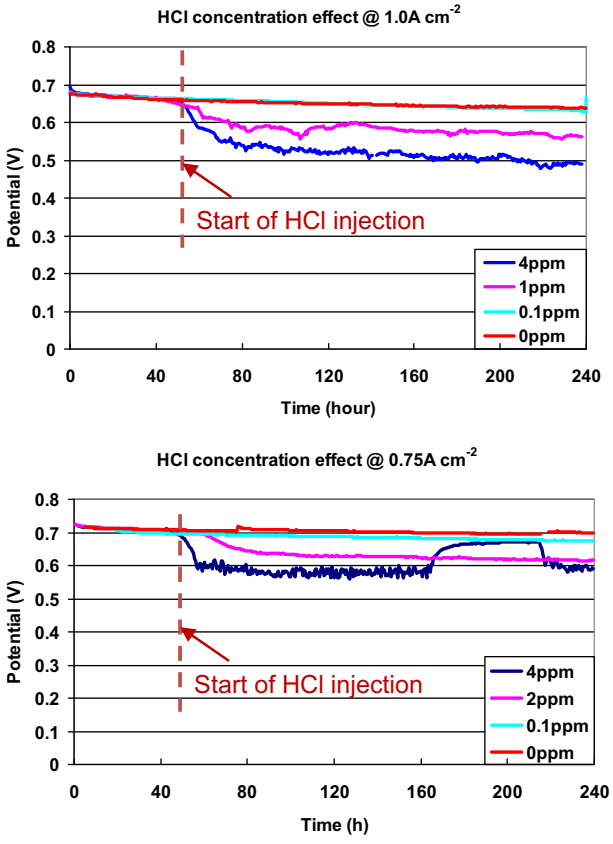

Fig. 1. Cell voltage vs. time curves collected at various HCl concentrations at two current densities. Other operating conditions are as listed in Table 1. Note: the large voltage increase during the 4 ppm HCl contamination test at 0.75 A cm^{-2} was a recovery test.

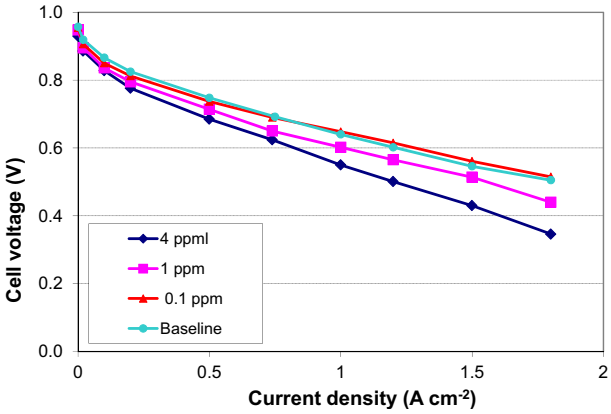

Fig. 2. Polarization curves collected at the EOT of contamination tests conducted at 1.0 A cm^{-2} with various HCl concentrations. Other operating conditions are as listed in Table 1.

3.1.2. ECSA losses vs. HCl concentration

Using CV measurements at both BOT and EOT, the cathode ECSAs and the ECSA losses ($ECSA_{BOT}$–$ECSA_{EOT}$) were estimated. As shown in Fig. 4, the presence of HCl caused a reduction in ECSA at all the tested concentration levels. In agreement with the performance impact, the ECSA decreased with increasing HCl concentration.

As discussed in our previous study [8], the presence of Cl^- reduces ECSA as a result of adsorption on Pt catalyst surface and enhanced Pt dissolution and subsequent Pt agglomeration due to the electrochemical formation of chloride complexes through the following reactions:

$$Pt + 4Cl^- \rightarrow PtCl_4^{2-} + 2e^- \quad (1)$$

$$Pt + 6Cl^- \rightarrow PtCl_6^{2-} + 4e^- \quad (2)$$

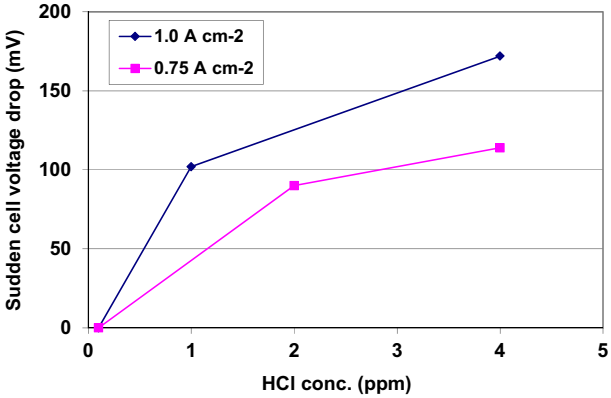

Fig. 3. Cell voltage sudden drop vs. HCl concentration at 1.0 and 0.75 A cm^{-2}. Other operating conditions are as listed in Table 1.

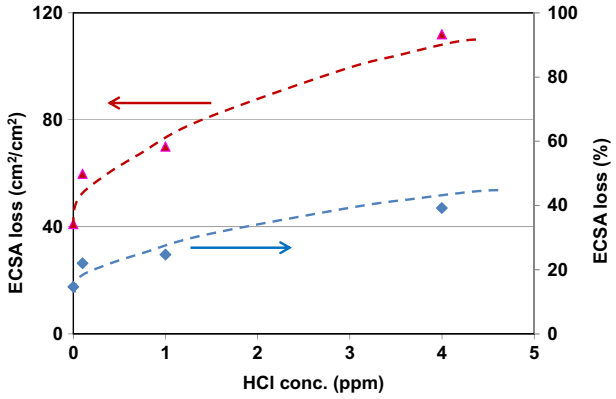

Fig. 4. Reduction of cathode ECSA vs. Cl^- level for contamination tests conducted at 1.0 A cm^{-2}. Other operating conditions are the same as for "effect of concentration 1" in Table 1.

The mechanism was confirmed by the Pt crystallite sizes estimated by XRD conducted on CCMs contaminated using various levels of HCl [8].

3.2. Effect of RH on Cl^- contamination

Changes in fuel cell operating conditions such as RH and temperature are often encountered in real fuel cell applications. Therefore, it is important to investigate how the change in fuel cell RH affects fuel cell performance and durability in the presence of HCl contamination. The effect of reactant inlet RH (40, 60, 80, and 100%) on HCl contamination was studied with 4 ppm HCl in the air stream at 1.0 A cm^{-2} (other conditions are shown in Table 1). As well, baseline tests were conducted under the same conditions.

3.2.1. Cell voltage vs. time

Fig. 5 shows the cell voltage vs. time for the four contamination tests (top), and the cell voltage vs. time for the corresponding baselines (bottom). The contamination tests at all RHs experienced an immediate sudden cell voltage drop with the introduction of HCl and then slowly reached a steady-state plateau performance. It should be noted that there were several interruptions during some of the contamination tests shown in Fig. 5 (top); however, these interruptions did not seem to affect the plateau cell performance.

To correlate the severity of HCl contamination effects with the fuel cell operating RH, the sudden drop in cell voltage are summarized as a function of RH in Fig. 6. As can be seen, the sudden drop in cell voltage decreased with increasing RH. The enhanced HCl contamination effect at reduced RH is likely related to the water content in the CCL and the Cl^- concentration in the liquid water phase. At the lowest tested RH (40%), the fuel cell had the lowest water content and thus the highest Cl^- concentration in the liquid phase, resulting in the highest surface coverage by Cl^- adsorption on the Pt surface. As a result, the cell voltage experienced the largest performance drop. The sudden drop became smaller as RH increased from 40 to 100%. It was also noted that the sudden cell voltage drop at 80 and 100% inlet RH was similar. Based on calculations, a significant fraction of the CCL was over-saturated by liquid water even at an inlet RH of 80%, which suggests that the liquid water content in the CCL was not very different for both 80 and 100% inlet RH. Therefore, it was deduced that the CCL water content played a critical role in the HCl contamination effect.

3.2.2. ECSA loss vs. RH

The ECSA loss for the contamination test at each RH was normalized as shown in Eq. (3):

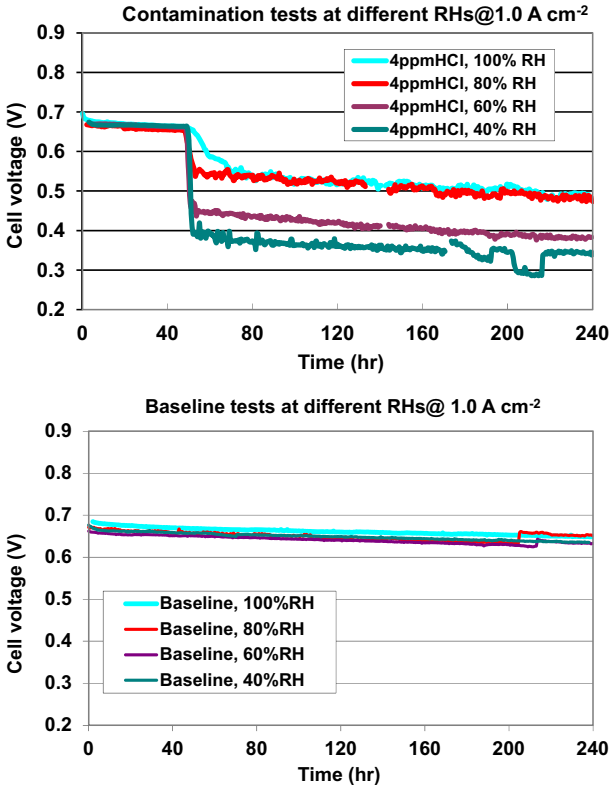

Fig. 5. Cell voltage vs. time curves collected during contamination tests at various RHs, with 4 ppm HCl in the air stream at 1.0 A cm^{-2}. Other operating conditions are as listed in Table 1.

$$\text{ECSA loss}_{\text{normallized}} = \text{ECSA loss}_{\text{actual}} - \text{ECSA loss}_{\text{baseline}} \quad (3)$$

The normalized ECSA loss plotted against the fuel cell RH, shown in Fig. 7. follows the same trend of 100% RH ≈ 80% RH < 60% RH < 40% RH as observed in the sudden cell voltage loss vs. RH shown in Fig. 6. The results supported the Cl^- adsorption and water content effect hypotheses presented above.

3.3. Effect of temperature on Cl^- contamination

Temperature is another important operating condition that is closely related to both fuel cell performance and the degradation rate. The effect of temperature on Cl^- contamination was

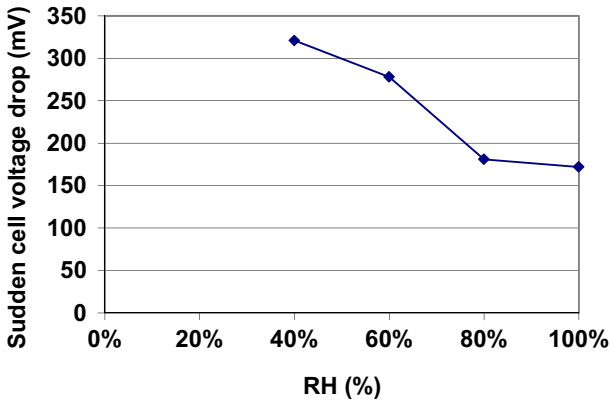

Fig. 6. Sudden cell voltage drop vs. RH for contamination tests conducted with 4 ppm HCl at 1.0 A cm^{-2}. Other operating conditions are as listed in Table 1.

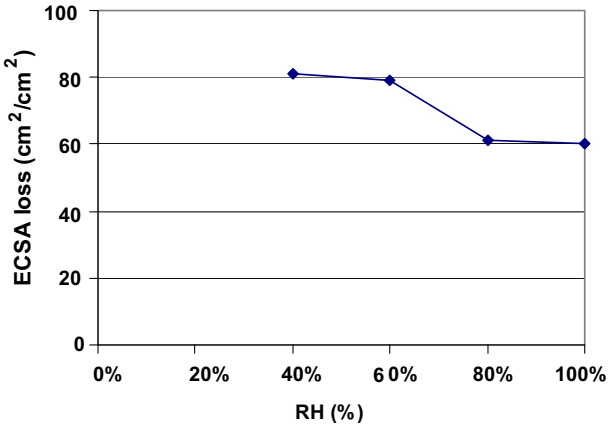

Fig. 7. Normalized ECSA losses for contamination tests with 4 ppm HCl at different RHs and 1.0 A cm^{-2}. Other conditions are as listed in Table 1.

investigated at various temperatures (40, 60 and 80 °C) with 4 ppm HCl and 80% RH at 1.0 A cm^{-2}.

The contamination results under different temperatures are displayed in Fig. 8 (top) while the corresponding baseline tests are shown in Fig. 8 (bottom). As shown in Fig. 8 (top), the cell performance change was found to display the same pattern at all temperatures during the contamination tests (i.e. a sudden decline in performance with the introduction of Cl^- followed by steady-state performance). However, the sudden cell voltage drop for the 40 °C test was not as immediate and sudden as for tests at the other two temperatures. In addition, as shown in Fig. 9 that summarizes the sudden voltage drop as a function of temperature, the severity of the contamination effect as measured by the sudden voltage

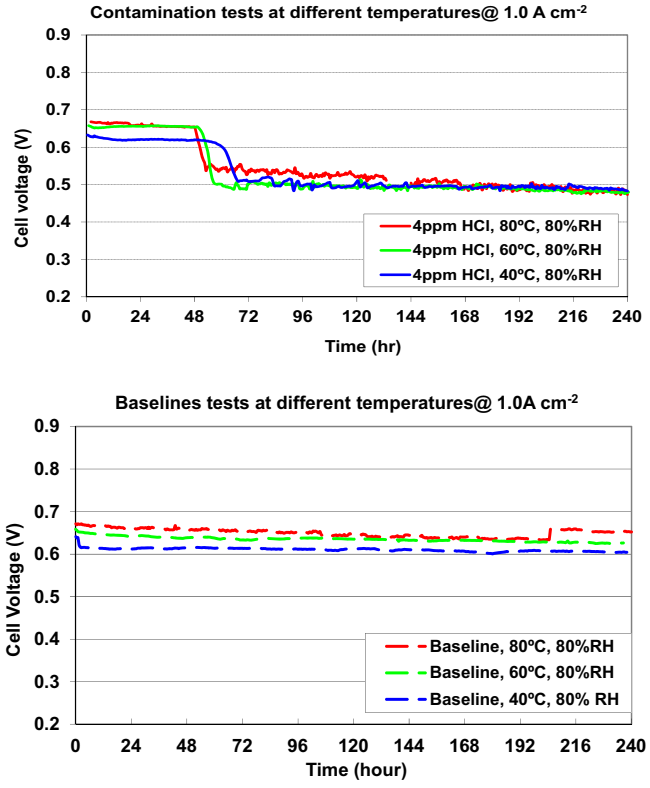

Fig. 8. Cell voltage vs. time curves collected during contamination tests at various temperatures, with 4 ppm HCl in the air stream at 1.0 A cm^{-2}. Other operating conditions areas listed in Table 1.

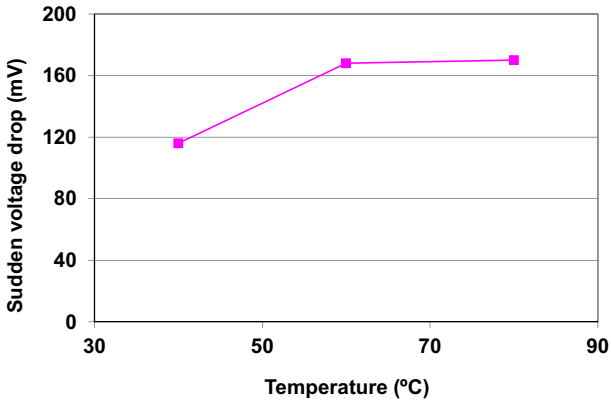

Fig. 9. Sudden cell voltage drop vs. temperature for contamination tests conducted with 4 ppm HCl at 1.0 A cm^{-2}. Other operating conditions are as listed in Table 1.

drop at 60 °C was much higher than that at 40 °C, but was very similar to that at 80 °C. This might be explained by the CCL liquid water content differences due to temperature differences and the counteracting effects of temperature on Cl^- adsorption and on the chemical formation of Pt-Cl complexes (shown in Eqs. (1) and (2)). Under the condition of constant inlet RH (80%) and pressure (25 psig), the evaporative effect of the liquid water generated from cathode reaction becomes stronger with increasing temperature; hence, the liquid water content in the CCL is expected to increase with decreasing temperature. Therefore, the observation that the 40 °C test showed the least amount of contamination effect was not surprising. Furthermore, the dependency of Cl^- adsorption and the chemical formation of Pt–Cl complexes on temperature is also a very important factor to consider. An increase in temperature would reduce the adsorption coverage of Cl^- on the catalyst surface, which would then result in a less severe contamination effect. Conversely, an increase in temperature would accelerate the chemical formation of Pt-Cl complexes and thus the agglomeration of Pt particles, which would result in a greater contamination effect. These two competing effects of temperature on Cl^- adsorption and on the formation of Pt–Cl complexes are likely part of the reason for the observed temperature effect.

3.4. Tests with MOT diagnostics

To further understand how the presence of HCl affects the ECSA during the course of contamination diagnostic tests, CV, OCV, hydrogen crossover current, and EIS measurements were conducted at MOT points during the contamination tests with 2 ppm HCl at 0.75 A cm^{-2} and 80% RH. Other operating conditions are listed in Table 1. For comparison, a baseline test with MOT diagnostics was also conducted in the absence of HCl under the same conditions.

3.4.1. Cell voltage vs. time

As shown in Fig. 10, the chosen diagnostic points were 0, 5, 23, 51, 117, and 217 h after Cl injection, and for comparison, the MOT points were controlled exactly the same for both the contamination and baseline tests. For the baseline test, it can be seen that the shutdown and restart for each of the MOT tests resulted in a temporary recovery in cell performance, which has been reported extensively in the literature [10,11]. For the contamination test, a similar temporary recovery was also observed for each shutdown and restart, but to a much greater degree than that of the baseline, suggesting that the change in cell voltage from the plateau value (around 0.5 V) during the normal contamination process to as high as 0.96 V during the OCV data collection, or as low as 0 V during CV measurements, led to at least partial recovery of the cell

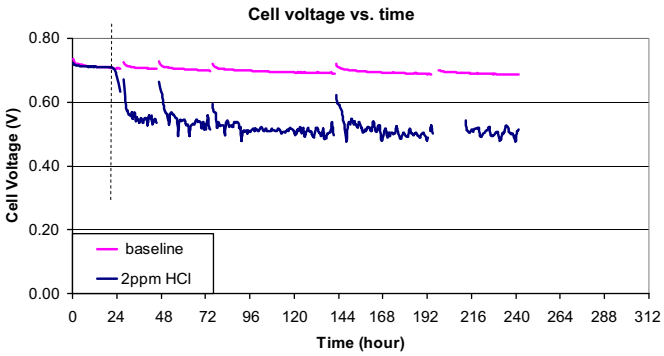

Fig. 10. Degradation curves for contamination and baseline tests conducted with mid-diagnostic measurements. HCl concentration: 2 ppm; RH: 80%; current density: 0.75 A cm^{-2}. Other conditions are as listed in Table 1.

performance loss caused by chloride contamination. However, once the HCl was re-introduced, the cell voltage returned to its plateau value.

3.4.2. EIS vs. time

The Nyquist plots for the baseline and contamination tests are shown in Fig. 11. It is important to note that the observed slight decreases in impedance after reaching a maximum at around 23 h is believed to be within experimental variation of the EIS technique. In conjunction with the observed cell voltage vs. time, the EIS results suggest that cell impedance is increased with HCl contamination until a plateau level is reached. In contrast, the Nyquist plots for the baseline underwent a rather steady and slow increase in the sizes of their two semi-circles. These observations point to the conclusion that the presence of HCl causes increases in both charge and mass transfer resistances, with the increase in charge transfer resistance being dominant, as can be seen from the fitted numerical values of the resistances (Fig. 12). The membrane resistance, however, is affected negligibly by the HCl contamination.

3.4.3. CV (ECSA) and hydrogen crossover vs. time

At each MOT point, LSV and CV were performed to determine the change in hydrogen crossover current and ECSA. The changes in hydrogen crossover current over time for both the baseline and the

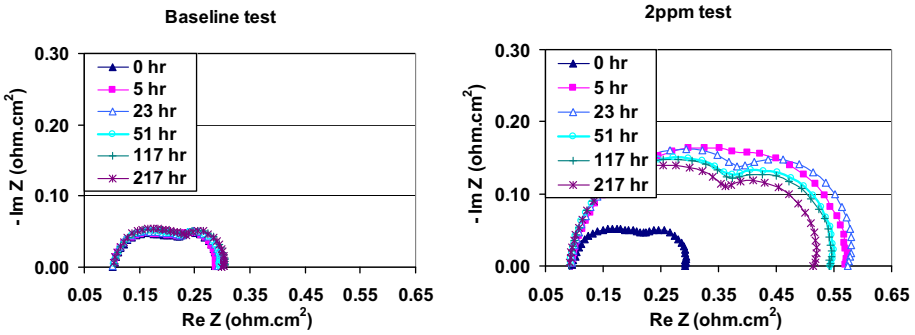

Fig. 11. Nyquist plots for the contamination test (2 ppm HCl) and baseline test, with mid-diagnostics at 80% RH and 0.75 A cm^{-2}. Other operating conditions are as listed in Table 1.

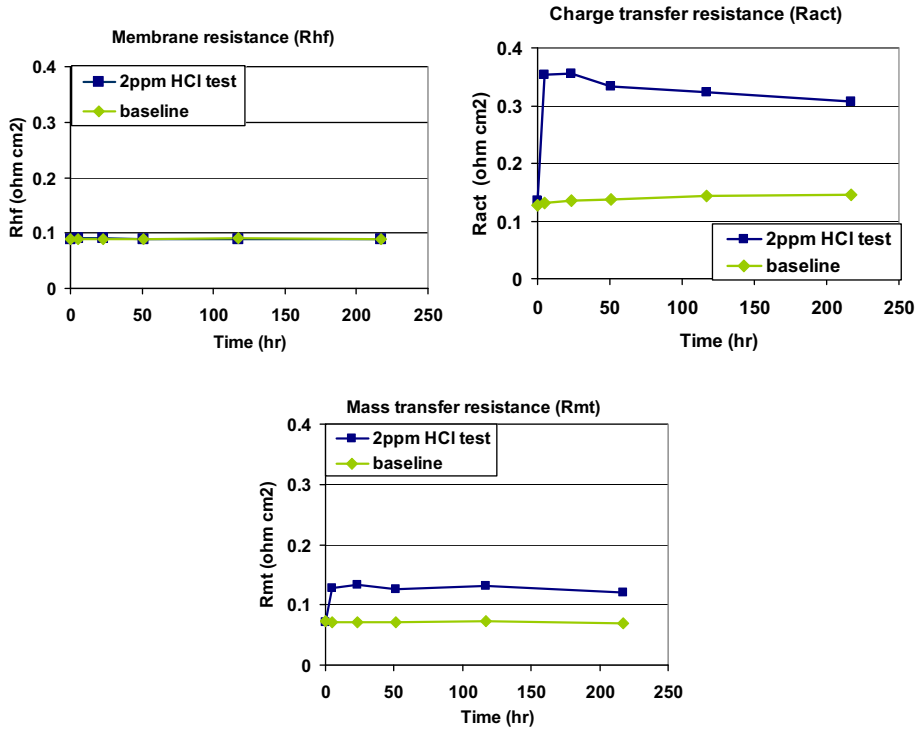

Fig. 12. Fitted individual resistances as a function of time for the contamination test (2 ppm HCl) and baseline test, with mid-diagnostics at 80% RH and 0.75 A cm^{-2}. Other operating conditions are as listed in Table 1.

Table 2
Hydrogen crossover current densities measured during the 2 ppm HCl contamination test with MOT diagnostics.

Contamination testing time (hr)	H_2 crossover current measured at 0.5 V (mA cm^{-2})
0	7.93
5	7.28
23	8.61
51	7.59
117	8.37
217	8.14

contamination tests were not significant over all MOT points (Table 2). However, the ECSA changed significantly over time for both baseline and contamination, and the change in ECSA over time was more dramatic for contamination. Fig. 13 compares the cyclic voltammograms obtained at 51 h for baseline and for contamination with 2 ppm HCl. Evidently, not only did the H-desorption and H-adsorption peaks become smaller in the presence of HCl, leading to reduced ECSA, the PtO/Pt redox peaks were also suppressed and shifted to the left. This suppression was also observed in our previous study using EQCM [9]. As discussed earlier, adsorption of Cl^- on the catalyst surface (thereby blocking the active sites) and enhanced Pt dissolution were believed to be the reason for the reduced ECSA.

The ECSA vs. time for the baseline and contamination tests are shown in Fig. 14. It is clear that with 2 ppm HCl injection, the ECSA decrease was much higher, than the change observed for the baseline. In addition, the difference in the ECSA between the baseline and the contamination tests was more significant during the first 24 h and then started to level off for the duration of the test. This implies that the contamination due to Cl^- adsorption and site-blocking on the catalyst surface started to occur at the beginning of the Cl^- injection; then, after a period of time, Cl^- adsorption reached a pseudo-equilibrium stage, leading to a similar rate of ECSA reduction in the contamination test and the baseline test, as can been seen from Fig. 14. It should be noted that this pseudo-equilibrium state could be disturbed by a change in cell voltage, as discussed earlier and also as seen from the temporary performance recovery shown in Fig. 10. But once the same concentration of HCl was resumed in the air stream, the Cl^- adsorption pseudo-equilibrium state was also resumed, and the cell performance went back down to its plateau value.

3.4.4. OCV vs. time

Fig. 15 shows the OCVs collected for both the contamination and the baseline tests. It can be seen that the presence of 2 ppm HCl in the air stream significantly affected the OCV values during dynamic operation, in comparison to the baseline. It has been reported [12] that deviation of the actual OCV value (around 0.96 V for a normally operated fuel cell) from its thermodynamic potential of 1.23 V is caused by two factors: hydrogen crossover from the anode side to the cathode side, and (the major factor) the so-called mixed potential caused by oxidation of Pt (the thermodynamic potential for Pt oxidation is 0.88 V) in the presence of O_2 to form a mixture of PtO and Pt instead of pure Pt. In other words, the actual OCV of the Pt electrode in the presence of O_2 is a mixed value of the potentials for the redox reactions of O_2/H_2O and PtO/Pt without any other contaminants present. As shown in Fig. 13, in the presence of 2 ppm HCl, the CV peaks of PtO/Pt were shifted, which might lead to a much lower OCV potential for Pt oxidation than its thermodynamic value of 0.88 V. In addition, the formation of Pt-Cl complexes in the presence of Cl^-, as shown in Eqs. (1) and (2), would add another contributor to the mixed potential. Since no significant change in hydrogen crossover current was observed in the baseline test, the results suggest that the Cl^--affected mixed potential is responsible for the observed reduction in OCV.

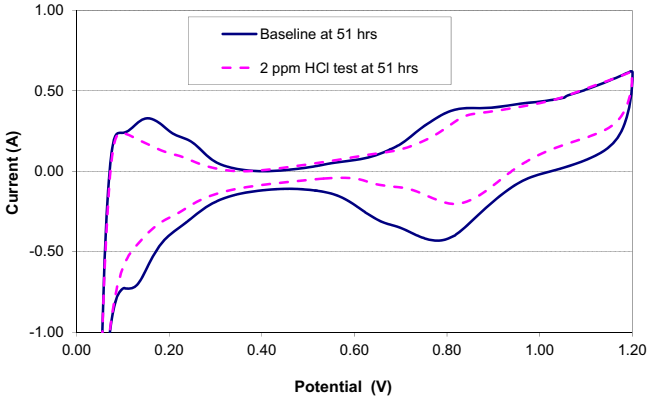

Fig. 13. CVs for the baseline and contamination (2 ppm HCl) tests measured at the mid-test point of 51 h. Operating conditions are as listed in Table 1 (test with MOT diagnostics).

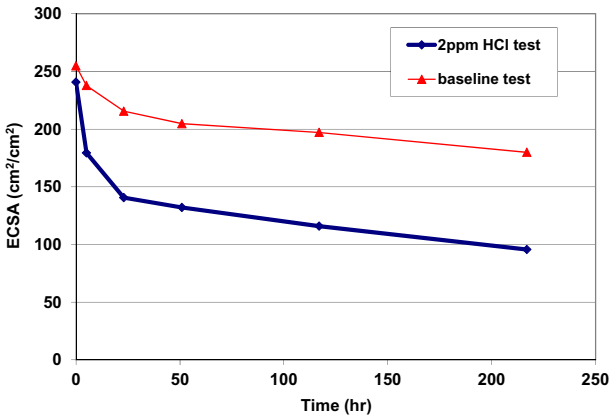

Fig. 14. ECSA vs. time for the contamination test (2 ppm HCl) and baseline test, with mid-diagnostics at 80% RH and 0.75 A cm^{-2}. Other operating conditions are as listed in Table 1.

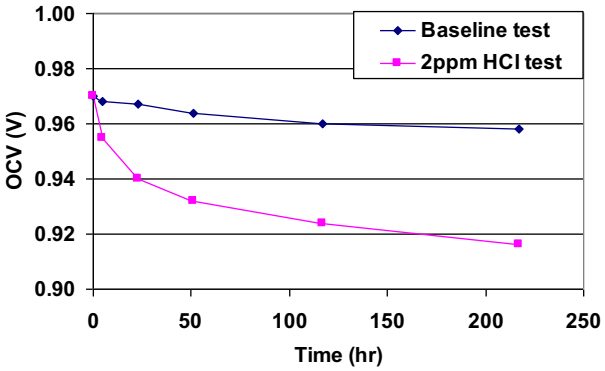

Fig. 15. OCVs vs. time for the contamination and baseline tests with mid-diagnostic tests, using 2 ppm HCl at 0.75 A cm^{-2} and 80% RH. Other operating conditions are as listed in Table 1.

4. Conclusions

The effects of trace levels of Cl^- in the air stream on PEM fuel cell performance and durability were studied with various levels of HCl concentration under different operating conditions. When the cathode of the PEM fuel cell was subjected to Cl^- at concentrations as low as 1 ppm, the cell suffered from a sudden performance loss

which levelled off with prolonged contamination. At a Cl^- concentration of 0.1 ppm, the cell performance did not experience this behaviour and exhibited a rather steady decay that was faster than that of the baseline. Operating conditions, such as current density, RH, and temperature, were found to have a significant impact on the severity of the chloride contamination effect. It was concluded that the contamination severity was worse with an increase in both current density and Cl^- concentration and a decrease in reactant RH. The influence of temperature on the chloride contamination effect was more complicated. As the temperature decreased from 80 °C to 60 °C, the sudden cell voltage drop did not change much. However, as the temperature decreased further from 60 °C to 40 °C, the sudden cell voltage drop was much lower.

measurement performed during the contamination tests showed that chloride contamination mainly caused increases in charge transfer resistance and mass transfer resistance but not in membrane resistance, and the increase in charge transfer resistance was dominant. CV measurements conducted at both BOT and EOT showed that the presence of chloride in the air stream significantly reduced the ECSA.

References

[1] S. Zhang, X.-Z. Yuan, H. Wang, W. Mérida, H. Zhu, J. Shen, S. Wu, J. Zhang, International Journalof Hydrogen Energy 34 (2009) 388–404.
[2] S. Ali, Q. Li, C. Pan, J.O. Jensen, L.P. Nielsen, P. Moller, International Journal of Hydrogen Energy 36 (2011) 1628–1636.
[3] T.J. Schmidt, U.A. Paulus, H.A. Gasteiger, R.J. Behm, Journal of Electrochemical Chemistry 508 (2001) 41–47.
[4] W. Yan, H. Chu, Y. Liu, F. Chen, J. Jang, International Journal of Hydrogen Energy 36 (2011) 5435–5441.
[5] K. Matsuoka, S. Sakamoto, K. Nakato, A. Hamada, Y. Itoh, Journal of Power Sources 179 (2008) 560–565.
[6] A.P. Yadav, A. Nishikata, T. Tsuru, Electrochimica Acta 52 (2007) 7444–7452.
[7] A. Zolfaghari, B.E. Conway, G. Jerkiewicz, Electrochimica Acta 47 (2002) 1173–1187.
[8] H. Li, H. Wang, W. Qian, S. Zhang, S. Wessel, T.T.H. Cheng, J. Shen, S. Wu, Journal of Power Sources 196 (2011) 6249–6255.
[9] A. Lam, H. Li, S. Zhang, H. Wang, D.P. Wilkinson, S. Wessel, T.T.H. Cheng, Journal of Power Sources 205 (2012) 235–238.
[10] S. Kundu, M. Fowler, L. Simon, R. Abouatallah, Journal of Power sources 182 (2008) 254–258.
[11] S. Zhang, X.-Z. Yuan, J.N.C. Hin, H. Wang, J. Wu, K.A. Friedrich, M. Schulze, Journal of Power Sources 195 (2010) 1142–1148.
[12] J.P. Chevillot, J. Farcy, C. Hinnen, et al., Journal of Electroanalytical Chemistry 64 (1) (1975) 39–62.